

A Geodetic Strain Rate Model for the Pacific-North American Plate Boundary, Western United States

Corné Kreemer¹William C. Hammond¹Geoffrey Blewitt¹Austin A. Holland²Richard A. Bennett²¹Nevada Bureau of Mines and Geology,
University of Nevada Reno²Department of Geological Sciences,
University of Arizona

2012

SUMMARY

This map presents a model of crustal strain rates derived from Global Positioning System (GPS) measurements of horizontal station velocities. The model indicates the spatial distribution of deformation rates within the Pacific-North America plate boundary from the San Andreas fault system in the west to the Basin and Range province in the east. As these strain rates are derived from data spanning the last two decades, the model reflects a best estimate of present-day deformation. However, because rapid transient effects associated with earthquakes (i.e., postseismic deformation resulting in curvature of the GPS time-series) have been removed from the GPS data, these strain rates can be considered representative of the long-term, steady-state, deformation associated with the accumulation of strain along faults. This model is useful for both seismic-hazard and geodynamic studies to understand the activity rates of (known and unknown) faults and the plate tectonic boundary and buoyancy forces that cause the deformation, respectively. In more slowly deforming areas we expect fewer, smaller earthquakes and infrequent large earthquakes will have a much longer recurrence time compared to those in rapidly deforming areas.



GPS stations: Continuous station (above left), Campaign station (above center) and UNR "MAGNET" station (above right).

GPS DATA

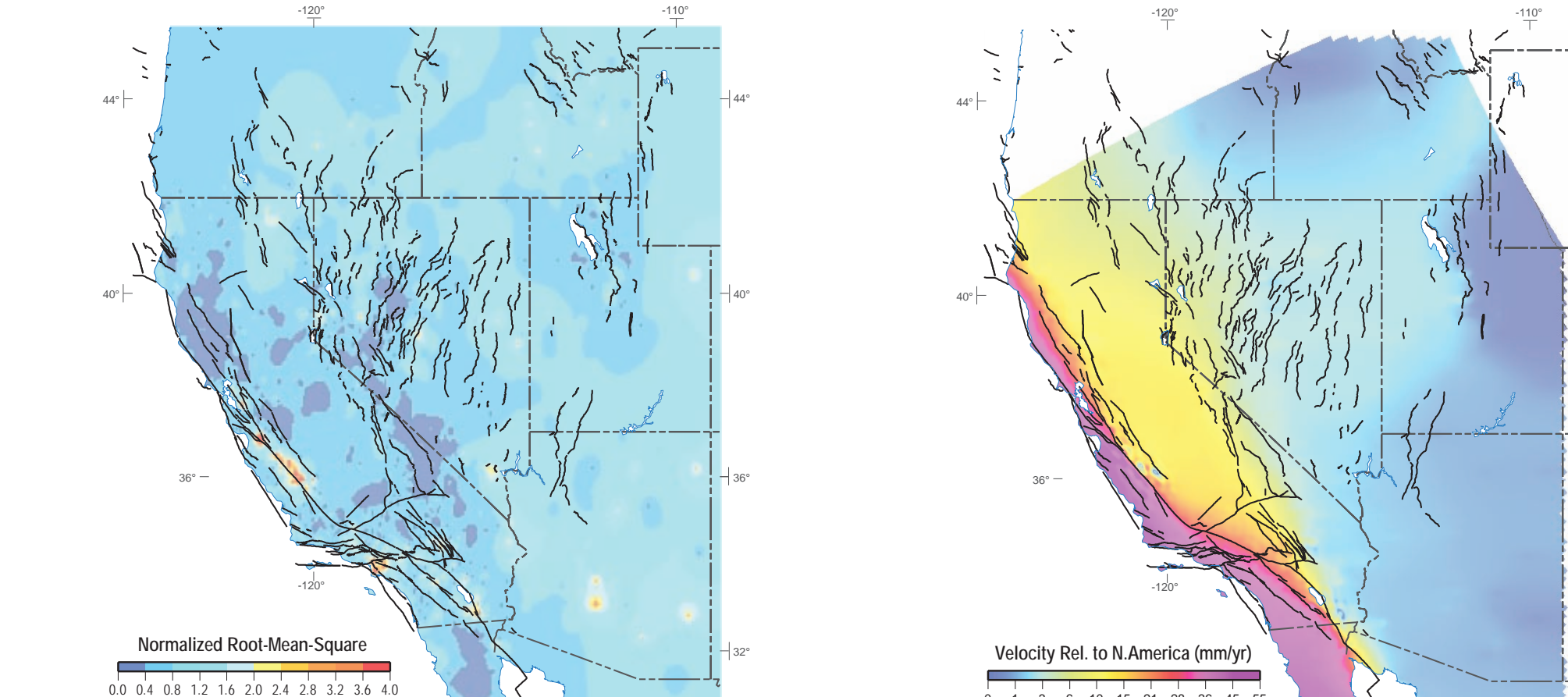
The GPS velocities were compiled specifically for this study. Of the total 2,846 velocities used in the model, 1,197 were derived by the authors, and 1,649 were taken from (mostly) published results. The velocities derived by the authors (the "UNR solution") were estimated from GPS position time-series of continuous and semi-continuous stations for which data are publicly available. We estimated ITRF2005 positions from 2002 to 2011.5 using JPL's GPSV-OASIS II software with ambiguity resolution applied using our custom Ambizap software. Only stations with time-series that span at least 2.25 years were considered. We removed from the time-series continental-scale common-mode errors using a spatially-varying filtering technique. Velocity uncertainties (typically 0.1–0.3 mm/yr) assume that the time-series contain flicker plus white noise. We used a subset of stations on the stable parts of the Pacific and North American plates (far from the plate boundaries) to estimate the Pacific-North American pole of rotation. This pole is applied as a boundary condition to the model, and the North American-ITRF2005 pole was used to rotate our velocities into a North America-fixed reference frame. We did not include parts of the time-series that show curvature due to post-seismic deformation after major

earthquakes and we also excluded stations whose time-series display a significant unexplained non-linearity or that are near volcanic centers. Transient effects longer than the observation period (i.e., slow viscoelastic relaxation) were left in the data. We added to the UNR solution velocities from published studies (Chang et al., 2006; Freymueller et al., 1999; Hammond and Thatcher, 2004, 2005, 2007; Lyons et al., 2002; Payne et al., 2008, 2012; Poland et al., 2006; Shen et al., 2011; Spinkler et al., 2010; Svarc et al., 2002; Titus et al., 2011; Williams et al., 2008) and those from an unpublished study for Arizona. The velocities were transformed onto the UNR solution's reference frame by estimating and applying a translation and rotation that minimizes velocity differences at collocated stations. We removed obvious outliers and velocities in areas that we identified to undergo subsidence likely due to excessive water pumping (e.g., California's Great Valley). All velocities used in the model are shown on map (velocities less than 4.5 mm/yr are saturated such that the vector head is shown irrespective of rate). More details can be found in Kreemer et al. (2012).

MODELING DETAILS

For the strain rate calculations, we excluded GPS stations with anomalous vertical motion or annual horizontal velocities, which are indicators of local site instability. First, we used the stations from the UNR solution to create a Delaunay triangulation and estimated the horizontal strain rate components (and rigid body rotation) for each triangle in a linear least-squares inversion using the horizontal velocities as input. Some level of spatial damping was applied to minimize unnecessary spatial variation in the model parameters. The strain rates estimates were then used as a priori strain rate variances in

a method that fits continuous bi-cubic Bessel spline functions through the velocity gradient field while minimizing the weighted residuals to all velocities (Beavan and Haines, 2001; Haines and Holt, 1993). A minimal level of spatial smoothing of the variances was applied. The strain rate tensor model is shown on the main map as contours of the second invariant of the tensor, which is a measure of the amplitude of the coordinate-frame independent. Faults with known slip rates (Haller et al., 2002) are shown on top of strain rates contours. More details can be found in Kreemer et al. (2012).



Contour map of the normalized root-mean-square (RMS) between observed and calculated velocities. For areas covered areas the data are 10 times less standard deviations. Note the large result along the central San Andreas fault where the fault creeps and where the model can not accurately fit a step function in the velocity field. Results are clipped at coast.

Contour map of the amplitude of interpolated velocities relative to North America. Results are clipped at coast.

Signal-to-noise (SNR) ratio is defined as the ratio of second invariant of the strain rate over the a posteriori standard deviation. These values are strongly affected by the GPS station density and the precision of velocities. Everywhere where SNR < 1, the area could be considered rigid, within one standard deviation. Conversely, for areas that appear nearly rigid and where SNR > 1 (e.g., Arizona, eastern Nevada) strain rates may be much more localized (i.e., higher) than the model suggests. Results are clipped at coast.

BIBLIOGRAPHY

Beavan, J., and Haines, J., 2001. Contemporary horizontal velocity and strain rate fields of the Pacific-Australian plate boundary zone through New Zealand. *Journal of Geophysical Research*, v. 106, p. 741–770.

Chang, L. L., Smith, R. B., Weertman, D. M., and Harris, R. A., 2006. Contemporary deformation of the Wasatch Fault, Utah, from GPS measurements with implications for interseismic fault behavior and earthquake hazard. *Observations and kinematic analysis*. *Journal of Geophysical Research*, v. 111, B11405. doi:10.1029/2005JB004228.

Freymueller, J. T., Murray, M. H., Segal, P., and Castillo, D., 1999. Kinematics of the Pacific-North American plate boundary zone, northern California. *Journal of Geophysical Research*, v. 104, p. 7419–7441.

Haines, A. J., and Holt, W. E., 1993. A procedure for obtaining the complete horizontal motions within zones of distributed deformation from the inversion of strain rate data. *Journal of Geophysical Research*, v. 98, 12,097–12,082.

Haller, K. M., Wheeler, G. L., and Bukaleski, K. G., 2002. Documentation of changes in fault parameters for the 2002 National Seismic Hazard Maps—Continuum United States except California. Open-File Report 02-467.

Hammond, W. C., and Thatcher, W., 2005. Northwest Basin and Range tectonic deformation observed with the Global Positioning System, 1999–2003. *Journal of Geophysical Research*, v. 110, B10405. doi:10.1029/2005JB003678.

Hammond, W. C., and Thatcher, W., 2007. Crustal deformation across the Sierra Nevada, Northern Walker Lane, Basin and Range transition, Western United States, measured with GPS, 2000–2004. *Journal of Geophysical Research*, v. 112, B05411. doi:10.1029/2006JB004620.

Kreemer, C., Hammond, W. C., Blewitt, G., Holland, A., and Bennett, R. A., 2012. A high-resolution strain rate model for the southwestern United States: 1. GPS velocity strain rate field. *Journal of Geophysical Research*, in preparation.

Lyons, S. N., Bock, Y., and Sanowal, D. T., 2002. Creep along the Imperial Fault, southern California, from GPS measurements. *Journal of Geophysical Research*, v. 107, p. 2049. doi:10.1029/2001JB001063.

Payne, S. J., McCallery, R., and King, R. W., 2008. Strain rates and contemporary deformation in the Snake River Plain and surrounding Basin and Range and seismically. *Geology*, v. 36, p. 647–650.

Payne, S. J., McCallery, R., King, R. W., and Kattenhorn, S. A., 2012. A new interpretation of deformation rates in the Snake River Plain and adjacent basin and range regions based on GPS measurements. *Geophysical Journal International*, v. 189, 101–122. doi:10.1111/j.1365-2466.2012.02707.x.

Poland, M., Burgmann, R., Dzurman, D., Litwack, M., Mazararak, T., Owen, S., and Fink, J., 2006. Constraints on the mechanism of long-term, steady subsidence at Medicine Lake volcano, northern California, from GPS, leveling, and InSAR. *Journal of Volcanology and Geothermal Research*, v. 150, p. 55–78.

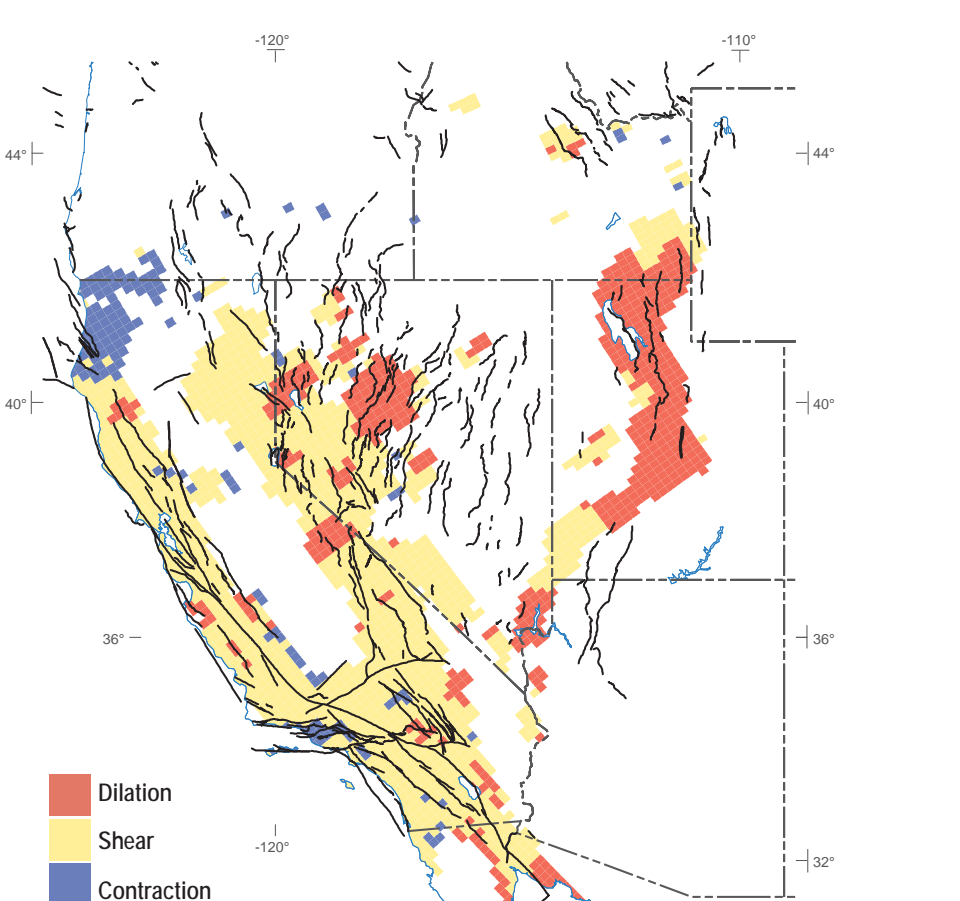
Shen, Z.-K., King, R. W., Agnew, D. C., Wang, M., Herring, T. A., Dong, D., and Fang, P., 2011. A unified analysis of crustal motion in Southern California, 1970–2004. The SCEC crustal motion map. *Journal of Geophysical Research*, v. 116, B11402. doi:10.1029/2011JB008549.

Spinkler, J. C., Bennett, R. A., Anderson, M. L., MOSE, S. F., Henshaw, S. J., and McCallery, A., 2010. Present-day strain accumulation and slip rates associated with southern San Andreas and eastern California shear zone faults. *Journal of Geophysical Research*, v. 115, B11407. doi:10.1029/2010JB007424.

Swain, J. L., Swain, J. C., Prescott, W. H., and Ramelli, A. R., 2002. Strain accumulation and rotation in western Nevada, 1993–2000. *Journal of Geophysical Research*, v. 107, p. 2090. doi:10.1029/2001JB000579.

Thur, S. J., Dixon, M., DeRosa, C., Hoff, B., Roseboom, F., and Burgmann, R., 2011. Geologic versus geodetic deformation adjacent to the San Andreas fault, central California. *Geological Society of America Bulletin*, v. 123, p. 794–820. doi:10.1130/B30150.1.

Williams, T. B., Kelsey, W. M., and Freymueller, J. T., 2006. GPS-derived strain in northernmost California: tectonic strain in the San Andreas fault system and convergence of the Sierra Nevada-Great Valley block contribute to southern Cascadia forearc contraction. *Tectonophysics*, v. 413, p. 171–184.



State	Surface Growth (acres/yr)
AZ	0.08
CA	-0.96
NV	0.20
UT	0.21

The negative value for California indicates shrinking, not growing.

GEODETIC VELOCITIES
RELATIVE TO NORTH AMERICA

10 MM/YR →

50 MM/YR →

→ Continuous GPS

→ UNR semi-continuous GPS

→ Other studies

→ Faults with known slip rates (Haller et al., 2002)

RATE OF DEFORMATION

2nd invariant strain rate tensor (10⁻⁹/yr)

0 2 6 14 30 72 136 264 520 1032 3600

0 20 40 60 80 100 120 140 160 Kilometers

Scale: 1:1,500,000 at latitude 39° Projection: WGS 1984 Web Mercator

General style of deformation for all areas where signal-to-noise ratio is less than 1. Results are spatially averaged. We define shear where the largest absolute principal value is less than twice the smallest absolute principal value. If not shear, we define dilation or contraction when the largest principal value is positive or negative, respectively. Results are clipped at coast.

